Electron Hopping through Films of Arenethiolate Monolayer-Protected Gold Clusters

W. Peter Wuelfing[†] and Royce W. Murray*[,‡]

Kenan Laboratories of Chemistry, University of North Carolina, Chapel Hill, North Carolina 27599-3290

Received: October 31, 2001; In Final Form: January 18, 2002

Electron hopping in films of arenethiolate (benzylthiolate, phenylethylthiolate, phenylbutanethiolate, and cresolthiolate) monolayer-protected cluster molecules (MPCs) is investigated through measurements of solid-state electronic conductivity. Electron donor−acceptor hopping rates between the Au cores of arenethiolate MPCs exceed those of previously studied solid-state alkanethiolate MPC films, but the electronic coupling term, $\beta = 0.8$ Å^{-1}, is nearly the same. Rate constants range from 10^8 to 10^{11} s^{-1} across the series of arenethiolate MPCs; for the case of cresolthiolate, the rate corresponds to a single molecule resistance of $\sim 10^7$ Ω/cresolthiolate ligand. The 4−8 kJ/mol activation-barrier energies for electron hopping are generally in line with the Marcus theory prediction. The low barrier energies and large rate constants arise from a combination of the low dielectric medium environment of the reactants (the MPC cores) and the partly aromatic tunneling bridges. The sharp increase in film conductivity upon substituting arenethiolate ligands for >50% of the hexanethiolates on a hexanethiolate-protected MPC suggests a percolation effect.

Introduction

The past decade has seen considerable interest in new kinds of nanostructures[1] based on molecular, semiconductor, and metallic nanoparticle components as pioneers in the continued miniaturization of electronic devices. To support these emerging concepts, the electron transfer (ET) dynamics in them must be understood because electron transport through the nanostructures is almost always involved.

We and others have reported[2] on the solid-state ET characteristics of Au nanoparticles passivated by tightly packed monolayers of alkanethiolate ligands, which we call monolayer-protected clusters, or MPCs.[3] The dimensions of the metallic cores of these nanoparticles lie near the transition between bulk metal and molecular properties. Like the better known semiconductor nanoparticles called "quantum dots",[4] MPCs can also exhibit size-dependent properties (quantized double-layer capacitance,[5] band gaps[6]). MPC materials hold promise for molecular electronic devices and other applications, given such characteristics and their tunable solid-state conductivity.[2]

The name "monolayer-protected cluster" emphasizes the general resistance, provided by the thiolate monolayer, to aggregation of the metal cores, even when all of the solvent has been removed. The ability to isolate MPCs as solids and redissolve them, like ordinary molecules, has facilitated both application of analytical tools for their characterization and elaboration of the monolayer's molecular structure.[3,7] Such studies have lead to compositional formulations of MPCs that express[3,8] average core sizes and numbers of core atoms and thiolate ligands per nanoparticle, like[8b] one of the nanoparticles in the present study: $Au_{309}[SCH_2(C_6H_5)]_{98}$. This (closed-shell) formulation is average because the nanoparticle samples generally exhibit some dispersity in core size. The nanoparticle dispersity feature is analogous to well-known aspects of polymer chemistry, where formulas are expressed as number- or weight-average molecular weights.

The electronic conductivity of solid-state MPC films reflects the facility of their electron transport, which, as in that of redox polymers,[9] occurs by an electron hopping, or electron self-exchange, mechanism. The MPC cores are treated as localized donor−acceptor sites on which the electronic charges reside, and the thiolate ligand shell, as a dielectric medium surrounding the cores that undergoes repolarization in the course of the electron transfer. The solid-state electron hopping conductivity, σ_{EL}, of thoroughly dried films of MPCs depends[2a] on (a) the charge carrier population, (b) the electronic coupling term, β, controlling the dynamics of electron core-to-core tunneling through the intervening thiolate monolayers and through the nonbonding contact between monolayers on adjacent MPCs, and (c) the activation-barrier energy of the electron transfer. The bimolecular aspects of charge transport were explored in ref 2a. Here, we further probe (b) and (c) by measuring solid-state conductivities of a set of recently prepared[8b] arenethiolate-MPCs that have 2.2−3.0 nm average core diameters. We aim to compare the arenethiolate-protected MPC conductivities and associated electron self-exchange rates with those[2a] of MPCs having alkanethiolate ligands (i.e., what is the effect of inserting aromatic segments into the MPC monolayers?). Others have shown that tunneling bridges (between electrodes and molecular sites) composed of alkane and fully conjugated linkers exhibit different β values ranging from 0.8 to 1.0 Å^{-1} and from 0.4 to 0.6 Å^{-1}, respectively.[10] Linker units composed of mixed saturated/conjugated chains have received less attention.[11] The monolayer ligands on MPCs used here have chains with mixed saturated/conjugated structures: cresolthiolate (SPhC), benzylthiolate (SCPh), phenylethylthiolate (SC2Ph), and phenylbutanethiolate (SC4Ph). The results show that the presence of the aromatic units increases the solid-state conductivity relative to that of alkanethiolate MPCs with similar Au core−core separations, but the electronic coupling term ($\beta_d = 0.8$ Å^{-1}) lies on the lower end of the range of known alkanethiolate values. The comparison includes accounting for differences

* Corresponding author. E-mail: rwm@email.unc.edu.
[†] Present address: Merck Manufacturing Division, Regulatory and Analytical Sciences, WP38-3, P.O. Box 4, West Point, Pennsylvania 19486.
[‡] University of North Carolina.

10.1021/jp013987f CCC: $22.00
Published on Web 02/22/2002

TABLE 1: Characterization of Arenethiolate-MPC Films

MPC[a]	av core diameter, nm [b]	calcd core edge−edge distance based on ligand head−head contact[c] 2*l*, Å	calcd MPC conc, M[d]	exptl core edge−edge distance 2*l*′, Å[e]	C_{EXPT}, exptl MPC conc, M[f]	*l*′/*l* [g]
$Au_{309}(S(CH_2)_4C_6H_5)_{143}$	2.2	19.2	0.032	14.2 ± 1.8	0.047 ± 0.006	0.74
$Au_{309}(S(CH_2)_2C_6H_5)_{98}$	2.2	13.6	0.049	10.2 ± 1.9	0.066 ± 0.012	0.75
$Au_{976}(SCH_2C_6H_5)_{363}$	3.0	10.6	0.033	10.6 ± 0.9	0.031 ± 0.003	1.0
$Au_{976}(SC_6H_4CH_3)_{363}$	3.0	12.0	0.030	6.6 ± 0.8	0.045 ± 0.004	0.55

[a] Average molecular formulas determined by combination of TEM average core diameters and thermogravimetric analysis. From ref 8b. [b] TEM average, ref 8b. [c] Determined from Hyperchem software. [d] From eq 3 using ∠. [e] From eq 3 using C_{EXPT}. [f] From pycnometry density measurement. [g] Ratio of experimental to calculated core edge−edge separations.

between arenethiolate and alkanethiolate ligand chains in the extent to which the nonbonding contact of monolayers involves interdigitation of chains on adjacent MPC cores, which determines the average distance between core edges.

In measuring the ability of molecular constructs to transport charge, experimental approaches can range from addressing single molecules to arrays of ordered molecules to random arrays of molecules. Elegant studies exist of the conductance of single benzenedithiol molecules using mechanical break-junctions.[1h] A significant body of theory also exists for the conductance of molecules interposed between metallic contacts (metal−insulator−metal or MIM).[1i,j] There is an enhanced ease and versatility of choice of monolayer organic tunneling barriers when the *average* conductances of large molecular monolayer populations are measured. Practical molecular electronic devices may in fact depend on average properties of molecular tunneling barriers. Average conductances have, for example, been determined[10e,f] for large populations of molecules in 2-D self-assembled monolayers on facing electrodes brought into contact.

The solid-state conductivities of films of MPCs are another example of average electron-hopping phenomena in large populations of molecules (the MPCs) lying between metal interfaces in which there is additionally some control over charge-carrier population.[2a] There is, however, an important difference between the MIM experiments referenced above and MPC conductivities in that electron transport through a film of MPCs occurs by successive electron donor−bridge−acceptor reactions where the MPC cores are the localized donor and acceptor sites. It is consequently more straightforward to convert solid-state electronic conductivities of nanoparticles to equivalent electron-hopping rate constants, k (s^{-1}), and to compare their thermal activation barriers to predictions[12] of contemporary electron-transfer theory. The resulting rate constants are quite large (as anticipated, given the low dielectric of the medium surrounding the electron-transfer centers), and the barrier energies are in reasonable agreement with those from the theoretical predictions. The barrier energies are slightly smaller than those[2a] of alkanethiolate MPCs.

We also estimate the effective resistances associated with single arenethiolate chains.

The transition from alkanethiolate to arenethiolate conductivity properties was additionally explored using MPCs with mixed monolayers of alkanethiolate and arenethiolate ligands. The MPCs are prepared by place (ligand)-exchange reactions.[13] The results show that significant increases in electronic conductivity accompany incorporation of >50% portions of arenethiolate ligands in a monolayer, suggestive of the operation of some kind of percolation threshold in the conductivity pathways.

Experimental Section

Chemicals. All chemicals were reagent grade and used as received.

Synthesis. MPCs were made using a 3:1 thiol/Au reactant mole ratio as described previously.[3a,8a,14] The Brust reaction[14] produces MPCs by a core nucleation−growth−passivation sequence whose details are poorly delineated. Briefly, $HAuCl_4$ is transferred from water into toluene by a quaternary alkylammonium phase-transfer agent and an alkanethiol is added, forming a $(Au^{I}SCn)_x$ polymer, followed by addition of BH_4^- (again, phase-transferred). The previously determined[8] average core diameters (by transmission electron microscopy) and molecular formulas (assuming a truncated octahedral core geometry[6b,15]) are given in Table 1. Hexanethiolate $Au_{140}(C6)_{53}$ MPCs (average composition) used in the ligand-exchange reactions were similarly synthesized with a 3:1 thiol/Au molar ratio.

Ligand-Exchange Reaction. $Au_{140}(C6)_{53}$ MPC (150 mg, ∼4.45 μmol) and thiocresol (29 mg, 0.23 mmol—a 1:1 mole ratio with the C6 ligands on the MPC) were codissolved in 100 mL of THF in a round-bottom flask and stirred at room temperature for either 1, 2, or 3 days. Each product aliquot (33 mL) was evaporated under vacuum in a round-bottom flask, and the solid was collected and washed on a medium-porosity frit with ∼500 mL of acetonitrile. ^{1}H NMR spectra (absence of sharp peaks[8a]) demonstrated the removal of all nonligated thiols. The ^{1}H NMR peak-area ratio of methyl (0.9 ppm) to phenyl (7.1 and 7.4 ppm) in the disulfide solution resulting from I_2 decomposition[3b] of the MPCs in CD_2Cl_2 gave the exchange percentage. Thermogravimetric analysis yielded the overall organic content. *Average* molecular formulas thus determined are 14% exchange, $Au_{140}(C6)_{44}(SPhC)_7$; 44% exchange, $Au_{140}(C6)_{35}(SPhC)_{27}$; and 57% exchange, $Au_{140}(C6)_{21}(SPhC)_{28}$. While a 3:1 thiol/Au mole ratio typically gives MPCs with an average Au_{140} core size (TEM measurements), the larger number of ligands on the 44% exchanged material suggests that the average core size may be smaller there (these individual preparations were not measured by TEM).

Electronic Conductivity. Electronic conductivities were measured on solid-state MPC films on interdigitated array electrodes (IDAs) (see the cartoon in Figure 1) obtained from Microsensor Systems, Inc. (SAW-302, 50 Au fingers, 15-μm finger width, 15-μm gap between fingers, 4800-μm finger length, 0.1-μm finger height). When calculating conductivity, the IDA finger walls are treated as parallel plate electrodes, with the total electrode area (A_{total}) being that of the fingers ($A_{fingers}$) facing one another across the IDA gaps:

$$A_{total} = A_{fingers}(N - 1) \quad (1)$$

where N equals the number of IDA fingers. The geometric cell constant of the IDA (gap distance (cm)/A_{total} (cm^2)) is 6.25 cm^{-1}. The MPC films were cast onto the IDA from three drops of a solution of ∼20 mg of MPC/0.1 mL of toluene and air-dried. The film thickness, ∼10−15 μm by stylus profilometry (Tencor

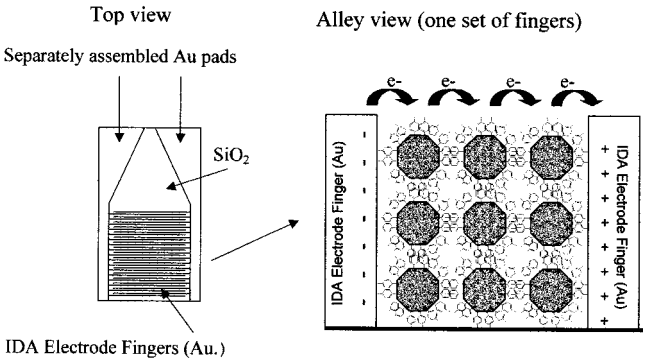

Figure 1. Cartoon of an interdigitated array electrode (IDA) from above (left) and from an alley view through an MPC down the interfinger gap (right, not to scale).

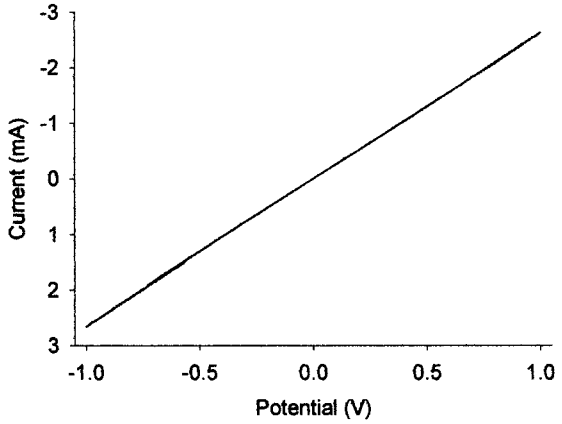

Figure 2. Current−potential response of a film of cresolthiolate (SPhC)-MPC (50 °C) on an IDA electrode.

Alpha-Step 100), is much greater than the IDA finger height. Conductivities for films from two versus three evaporated droplets were identical. The coated IDAs were placed on a temperature stage in a vacuum chamber (Fisher Maxima C pump) and held at 30 °C for ∼10 min to evaporate the toluene solvent. The temperature was lowered to an initial value of −50 °C and raised in 10 °C increments to 50 °C, equilibrating for 20 min at each temperature before measuring the conductivity. An initial measurement taken at 30 °C (before cooling) was usually within 5% of the conductivity at the same temperature as that measured in the heating cycle. Conductivities were measured[2a,16] using linear (ΔE) potential sweeps; the current−potential response is shown in Figure 2. At larger potential bias values, the current response curves upward, as shown in earlier studies,[2a,16] but in the ±200 mV portion of the curve, the response is linear.

$$\sigma_{EL} = \frac{d\Delta i}{A_{total}\Delta E} \qquad (2)$$

The slope $\Delta i/\Delta E$ (Ω^{-1}) gives conductivity; d = IDA gap (cm), and A_{total} is from eq 1. Potential scans were started at 0 V bias and swept over ±1 V at 100 mV/s; the results were unchanged at 5, 10, and 200 mV/s. Generally, two or three measurements were taken at each temperature, with <2% variation.

MPC Concentration. The solid-state concentrations of MPCs determine their average core edge−edge separations (l'), which are important for analysis of the electron hopping and for how ligands pack between adjacent MPC cores. For alkanethiolate MPCs, monolayer chains from adjacent MPCs tend to interdigitate, as shown both experimentally[2,3a] and theoretically.[15]

Arenethiolate MPC concentrations (Table 1) were calculated from pycnometrically[2a] determined densities divided by average MPC molecular weights. Equation 3 relates the apparent ligand chain length (l'') to the experimental MPC concentration (C_{expt}, M) and the MPC core radius:

$$C_{expt} = \frac{0.7(10^3)}{\frac{4}{3}\pi(r_{core} + l'')^3 N_A} \qquad (3)$$

N_A is Avogadro's number and 0.7 is the fill factor for a hexagonally close packed film, and the 10^3 factor converts dimensions to molar concentrations. Experimental MPC core edge−edge distances $2l''$ can be calculated by calculating l'' from eq 3. (Most of the experimental uncertainty in l'' is associated with the pycnometric experiment.) These are compared in Table 1 to core edge−edge distances calculated assuming *no* intercalation (i.e., $2l$, where the MPC core edges are separated by ligand *head−head* contact between fully extended chains of length l-(calculated by modeling software[17]). The ratio (Table 1) l''/l is less than unity for three of the four arenethiolate MPCs, reflecting presumably either chain interdigitation (like alkanethiolate-protected MPCs) or some other kind of chain distortion.

Electrochemistry. Core charge state can influence solid-state conductivity.[3a] Rest potentials[2a,18] (E_{rest}) of MPC solutions in CH_2Cl_2 were accordingly measured for the arenethiolate and $Au_{140}(C6)_{53}$ MPCs. The indicator electrode was a 0.6-mm diameter Pt disk and a Ag/Ag^+(0.01 M in CH_3CN) electrode, the reference (potential is ca. −50 mV vs the Ag/AgCl wire quasi-reference electrode used previously[2a]). E_{rest} of arenethiolate-MPC solutions was generally ca. −0.25 V vs Ag/Ag^+, near the potential-of-zero charge previously assigned[5d] to alkanethiolate-MPCs. We assume that arenethiolate E_{PZC} values are the same. E_{rest} for the as-prepared Au_{140} MPCs was ca. −0.61V vs Ag/Ag^+, implying the presence of a residual reductive charge, namely, an $MPC^{2-/1-}$ mixture.

Thermogravimetric Analysis. Thermogravimetric analyses (TGA) were obtained with a Seiko Instruments RTG 220 robotic TGA.

Results and Discussion

Arenethiolate-MPC Electron-Hopping Conductivities. Electron hopping in MPC films (cartoon in Figure 1) is a thermally activated process in which the thiolate monolayer electron-tunneling barrier properties appear in the conductivity (Ω^{-1} cm^{-1}) preexponential { }term:[2a]

$$\sigma_{EL}(\delta,T) = \{\sigma_0 \exp[-\beta_d\delta]\} \exp[-E_A/RT] \qquad (4)$$

β_d is the electron-tunneling coefficient ($Å^{-1}$), δ is the average MPC core edge−edge distance (Å; $2l''$), E_A is the activation-barrier energy (kJ/mol), and T is the temperature (K). Activation plots for electronic conductivity are given in Figure 3; see Table S-1 for the detailed data. The plots are fairly linear,[19] with small activation-barrier energies ranging from 4 to 9 kJ/mol (Table 2). As we expected, the conductivities (Table 2, σ_{EL} 30 °C) of arenethiolate-protected MPCs *increase with decreasing content of saturated units in the monolayer*. The conductivities of most are larger than those of MPCs with exclusively hexanethiolate (C6) and butanethiolate (C4) monolayers (see comparison data[2a] in Figure 3).

First-order electron-hopping rate constants, k_{ET} (s^{-1}), can be estimated from nanoparticle film conductivities by assuming a cubic-lattice model, as has been done previously for redox

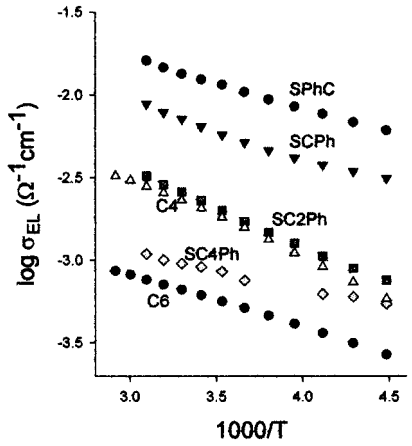

Figure 3. Arrhenius plot of electronic conductivities of arenethiolate-MPCs from the present study and selected alkanethiolate sample films from ref 2a ($Au_{309}(C6)_{92}$ and $Au_{309}(C4)_{92}$ average molecular formulas).

polymers and alkanethiolate-protected nanoparticles:[2a,9,20,21]

$$k_{ET}(s^{-1}) = \frac{6RT\sigma_{EL}}{10^{-3}F^2\delta^2 C_{expt}} \qquad (5)$$

R is the gas constant, F, the Faraday constant, and the other symbols, as above. This relation normalizes for nanoparticle concentration and associated core edge−edge distances, which is important because the arenethiolate-MPC samples have different average Au core sizes (Au_{309} and Au_{976} average composition) and core edge−edge distances. The essence of eq 5 is that electronic charge is localized on MPC cores as electron donor−acceptor reactants. Equation 5 also assumes implicitly that the carrier concentration equals the MPC core concentration, which, following our previous discussion[2a] of this point, is a reasonable assumption for the relatively large cores of the arenethiolate-protected nanoparticles. Results for electron-hopping rate constants (Table 2), which are *averages* given the above assumptions and the imperfect MPC monodispersity, range from 10^8 to 10^{11} s^{-1}, varying widely in a manner qualitatively consistent with the core−core separation. As noted in Figure 3, the electron-hopping rates exceed those of short chain alkanethiolate MPCs.

Equation 4 predicts an exponential dependence of electron-hopping rate constants on core edge−edge distance (δ or $2\prime\prime$, Table 1). The corresponding plot for the arenethiolate-protected MCPs, Figure 4 (upper curve, □), shows that log k_{EX} (30 °C) is only crudely linear with $2\prime\prime$. The correlation line gives an electronic coupling parameter of 0.77 $Å^{-1}$. Figure 4 (lower curve, ●) displays previous[2a] data for solid-state alkanethiolate-MPC films ($Au_{309}(Cn)_{92}$ average composition), by which the similarity in the two systems of decay of electron-hopping rates with distance is apparent despite the scatter in the arenethiolate data.

The obvious scatter in the arenethiolate-protected MPC distance dependency plot in Figure 4 (upper curve) is puzzling, contrasting with the relatively regular behavior of the alkanethiolate-protected MPC (Figure 4, lower curve). Figure 5 presents an alternative analysis of the arenethiolate-MPC rate constant results (left-hand axis), in which instead of the distance term of eq 4, we plot the number of saturated carbons between the sulfur and phenyl groups in the arenethiolate ligands. This number ranges from zero to four. The exponential dependence of both the electronic conductivity and rate constant that is the signature of a tunneling-controlled reaction rate now appears much more clearly than it does in Figure 4 (upper curve). A similarly linear plot and identical slope are obtained by plotting data (not shown) taken at −50 and 50 °C (i.e., the electronic coupling is independent of temperature, like that of the alkanethiolate-MPCs[2a]).

The analysis of Figure 5 and the generally parallel plots in Figure 4 emphasize that in monolayers where each chain structure contains a mixture of alkane and arene units the incremental attenuation of the electron-transfer rate is, nearly quantitatively, that characteristic of saturated carbon segments. Figure 5 emphasizes that, as a linking unit, the distance increment provided by the aromatic portion of the monolayers seems to be effectively "invisible". The slope of the plot, the saturated carbon unit-dependent electron-tunneling constant is 1.5/saturated unit. However tempting, it is unclear how this result for a mixed saturated/unsaturated monolayer may be converted to an electronic-coupling parameter. Additionally, the methyl unit on the $Au_{976}(SC_6H_4CH_3)_{363}$ MPC seems to be "bypassed" as a tunneling-barrier element, which is consistent with the intercalation analysis of Table 1 in which the tolylthiolate ligands appear to intercalate to fully one-half of their overall length.

The results for the arenethiolate-protected MPCs are quite different from those obtained on self-assembled monolayers by Cheng et al.,[11] who report a 3-fold *decrease* in the rate of electron transfer through the monolayers by replacing a methylene unit in the monolayer chain by an olefinic group. In the arenethiolate MPCs, the aromatic segment *enhances* the overall electron-hopping rate, as seen in Figure 4, by approximately an order of magnitude. This comparison also suggests that, like results from Slowinski et al.[10e] and Holmlin et al.,[10f] nonbonding contacts between monolayers that serve as tunneling bridges do not result in any large retardation of the overall electron-tunneling rate.

As a final note, core sizes of the longer chain length arenethiolate MPCs are smaller[8b] (Table 1). The preceding analysis accounted for core size in terms of its effects on MPC concentration and core edge−edge distances. Whether there are additional electron-transfer rate effects associated with MPC core size is as yet undiscovered. A previous study[2a] of alkanethiolate-protected MPCs revealed no clear additional core-size effects between $Au_{140}(C6)_{53}$ (average 1.6-nm diameter) and $Au_{309}(C6)_{92}$ (average 2.2-nm diameter).

Activation-Barrier Energies. Figure 3 yields activation-barrier energies (E_A) associated with electron hopping in the MPC films that are collected in Table 2. The results show that the barrier energies all lie within a factor of 2 of one another and that they are relatively small (0.04−0.09 eV). We have been interested in how readily, as a first approach to the chemistry of electron transfer between tiny pieces of metal (i.e., the Au cores), dielectric continuum theory[12] could predict activation-barrier energies in solid-state alkanethiolate-MPC films. Results with alkanethiolate-protected MPCs were encouraging.[2a,22] Marcus theory, as pertaining to MPC films, is based on repolarization of the organic dielectric continuum (the monolayers) between the Au cores, giving a free energy of activation (ΔG^*) that, absent any "inner sphere" effects, is

$$\Delta G^* = \frac{\lambda}{4} = \frac{e^2}{16\pi\epsilon_0}\left(\frac{1}{2r_1} + \frac{1}{2r_2} - \frac{1}{r}\right)\left(\frac{1}{\epsilon_{op}} - \frac{1}{\epsilon_s}\right) \qquad (6)$$

where λ is the "outer sphere" reorganizational barrier energy, r_1 and r_2 are the radii of neighboring MPCs (TEM-determined, average MPC radius), r is the center−center distance between

TABLE 2: Activation Energy and Conductivity Data for Arenethiolate-MPC Films

MPC	E_A, Arrhenius (kJ/mol)[a]	E_A, calcd (kJ/mol)[b] ($\epsilon_s = 3.9$)	E_A, calcd (kJ/mol)[b] ($\epsilon_s = 2.3$)	σ_{EL} (30 °C) (Ω^{-1} cm^{-1})[c]	k_{ET} (s^{-1})[d] cubic lattice
$Au_{309}(S(CH_2)_4C_6H_5)_{143}$	4.1 ± 0.4	4.1	0.2	1.5×10^{-4}	$2.6(\pm0.3) \times 10^{8}$
$Au_{309}(S(CH_2)_2C_6H_5)_{98}$	8.8 ± 0.2	3.9	0.2	2.6×10^{-3}	$6.1(\pm1.1) \times 10^{9}$
$Au_{976}(SCH_2C_6H_5)_{363}$	6.2 ± 0.6	2.7	0.1	7.2×10^{-3}	$3.3(\pm0.3) \times 10^{10}$
$Au_{976}(SC_6H_4CH_3)_{363}$	5.7 ± 0.2	2.6	0.1	1.3×10^{-2}	$1.1(\pm0.1) \times 10^{11}$

[a] From the higher temperature section of Arrhenius plots in Figure 3. [b] Calculated from eq 5. [c] From 30 °C linear potential sweeps of the different MPC films, as described in the Experimental Section. [d] Calculated from eq 5 using the σ_{EL} value from a 30 °C IDA current−potential curve.

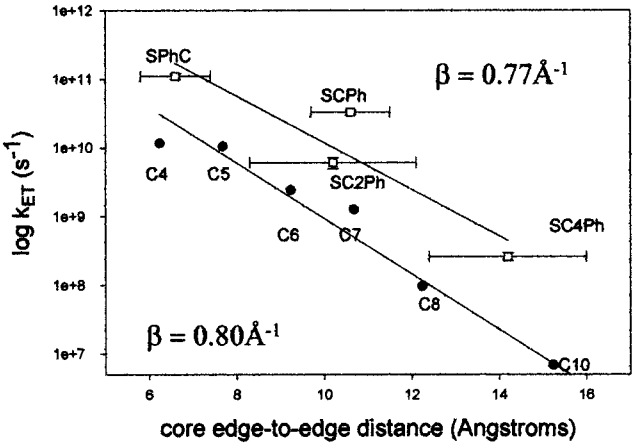

Figure 4. k_{ET}-based β_d plots for arenethiolate- and alkanethiolate-protected MPC films with similar core edge-to-edge distances.

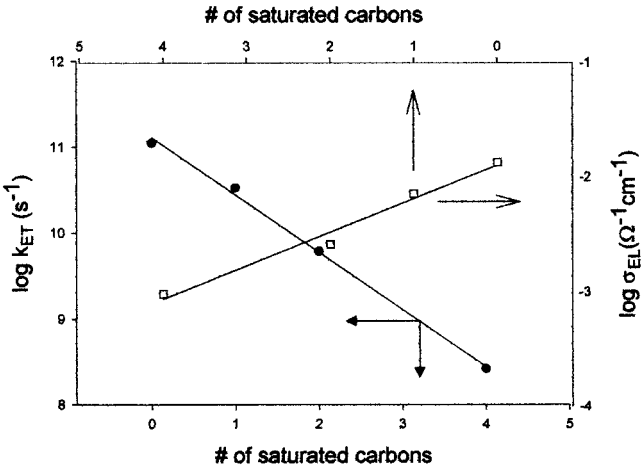

Figure 5. k_{ET} and σ_{EL} compared to the number of saturated carbon units between the aromatic component and the thiolate center.

Au cores (a function of the arenethiolate used), and ϵ_{op} and ϵ_s are the medium optical and static dielectric constants, respectively.

To calculate ΔG^* from eq 5, an ϵ_{op} value ([refractive index]^2) of 2.25 was taken from literature alkylarene values,[23] and the ϵ_s value was taken for phenylethylene (2.3) to represent the arenethiols. These constants and eq 5 produce barrier energies (Table 2) that are much smaller than the experimental ones. In a second set of calculations, we sought a value of ϵ_s producing general agreement with that (3.9) from experiments for MPCs made from phenylbutanethiol. It is notable that this ϵ_s value differs from the 2.3 phenylethylene value by a factor of 1.7, which is the same factor of difference seen by others[24] between dielectric constants measured on self-assembled alkanethiolate monolayers on a Au(111) electrode and those of bulk alkanethiols. For the other three ligands, the experimental data are generally somewhat larger (by about 2-fold) than data calculated

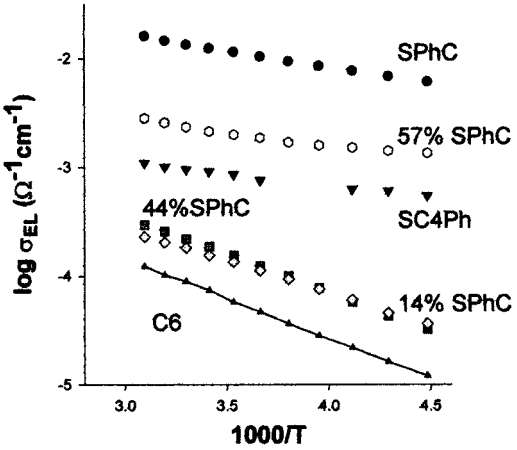

Figure 6. Arrhenius plots for mixed monolayer hexanethiolate/cresolthiolate-MPC films and selected arenethiolate and alkanethiolate films. The mixed monolayer MPC concentrations, ⁄″ core edge-to-edge distances, ⁄ fully extended[17] hexanethiolate chain length (normal to Au surface), and ⁄″/⁄ values are 17% cresolthiolate in monolayer (0.105 ± 0.010 M, 5.8 ± 0.5 Å, 7.7 Å, 0.75); 44% cresolthiolate in monolayer (0.182 ± 0.018 M, 3.5 ± 0.4 Å, 7.7 Å, 0.45); and 57% cresolthiolate in monolayer (0.094 ± 0.004 M, 6.3 ± 0.3 Å, 7.7 Å, 0.82).

using $\epsilon_s = 3.9$. This general level of agreement is about the same as that found[2a] for the alkanethiolate-protected MPCs. The small static dielectric-constant value that produces this level of agreement emphasizes that the observed electron-transfer rate constants are very large because of the low dielectric medium surrounding the Au core reaction centers. Also, in light of the various assumptions and uncertainties, which include those of monodisperse core size and uniform MPC packing in the film (necessary in the above calculations), we continue to see eq 5 as a useful tool in exploration of this new area of electron-transfer dynamics.

Studies of MPCs with Mixed Monolayers of Alkanethiolate and Arenethiolate Ligands. The substantial difference in electronic conductivites (e.g., electron-transfer rates) of MPCs with alkanethiolate versus arene−alkanethiolate monolayers (Figure 3) leads us to a few experiments exploring the properties of MPCs with monolayers containing mixtures of alkanethiolate and arene−alkanethiolate ligands. MPCs with mixed monolayers were readily prepared by place (ligand)-exchange[3] reactions between well-characterized hexanethiolate-protected MPCs ($Au_{140}(C6)_{53}$) and cresolthiol, as described in the Experimental Section. The place-exchange reaction between an incoming thiol ligand and a Au core-bound thiolate is thought to be an associative process.[25]

MPCs with mixed monolayers containing 14, 44, and 57% cresolthiolate ligands were prepared, and their conductivities were measured as a function of temperature, as shown in Figure 6. (Detailed data are in Supporting Information Table S-2, and conductivities of cresolthiolate, hexanethiolate, and butanethiolate MPCs are shown in Figure 6 for comparison.) The results show (as anticipated) that the conductivities of the mixed-

monolayer MPCs lie between those of cresolthiolate and hexanethiolate-protected MPCs and increase in order of the proportion of cresolthiolate ligands. What is notably interesting is that the 14 and 44% thiocresol-exchange MPCs display nearly identical σ_{EL} values, whereas the MPC with 57% cresolthiolate ligands exhibits a substantial jump in conductivity. The latter MPC exhibits, in fact, a conductivity greater than that of the most conductive alkanethiolate MPC (butanethiolate). These observations suggest that the mixed monolayer films display an "averaged" character in terms of the efficacy of electron tunneling through large populations of ligands. Also, the 57% material suggests that the averaging is weighted in terms of the efficiency of electron transport by tunneling through arenethiolate ligands, which leads to some kind of percolation threshold in the amount of those ligands. If electronic charge passed through the least resistive chains only, one would expect the 57%-exchanged MPC film (where the extent of exchange implies that there are cresolthiolate ligands on all core surfaces) and the cresolthiolate-MPC film to have a nearly identical Arrhenius plots. As mentioned above, the resulting conductivity, which is between the C6 and SPhC values, appears to be an average between the two. These results indicate that charge transfer in MPC films proceeds through many ligands, not simply the least resistive. Charge likely then tunnels through the chains in a fashion similar to that through a set of parallel resistors.

Molecular Resistances. It is interesting to cast the electron-transfer rate constants derived for reactions of these MPCs in terms of average molecular resistivity units (Ω) per MPC or monolayer ligand. The electron-transfer rate constant is related to MPC resistivity by

$$R_{CT,MPC} = \frac{(RT)N_A}{F^2 k_{ET}} \quad (7)$$

where $R_{CT,MPC}$ is the resistance to charge transfer of the molecular material between two individual MPC units (Ω), R and T are the gas constant and temperature (K), respectively, N_A is Avogadro's number, F is the Faraday constant, and k_{ET} is the first-order electron-transfer rate constant for MPC−MPC reactions. Equation 6 yields values of 6×10^8, 3×10^7, 5×10^6, and 2×10^6 Ω/MPC for the SC4Ph, SC2Ph, SCPh, and SPhC arenethiolate-MPCs, respectively. These values can be further broken down into resistances of individual alkanethiolate chains by modeling the junctions between individual MPC neighbors as parallel resistors that contain[26] between 10 and 20 chain contacts. This procedure yields molecular ligand resistances of 6×10^9, 3×10^8, 9×10^7, and 3×10^7 Ω/arenethiolate ligand for the ligands SC4Ph, SC2Ph, SCPh, and SPhC, respectively. Given the simplicity of this analysis, the correspondence of the result (3×10^7 Ω) for the cresolthiolate-ligand method to that from a previous report[1h] of the single-molecule resistance of the nearly identical molecule benzenedithiol ($\sim 2 \times 10^7$ Ω) is rather remarkable.

Acknowledgment. This work was supported in part by grants from the DOE and NSF. W.P.W. acknowledges a NASA graduate student research fellowship for financial support. We thank Professor Joseph DeSimone and Dr. Steve Gross (UNC-CH) for use of the TGA equipment.

Supporting Information Available: Supplementary Tables S-1, S-2, and S-3 give data for Figures 3 and 6. This material is available free of charge via the Internet at http://pubs.acs.org.

References and Notes

(1) (a) Tour, J. M. *Acc. Chem. Res.* **2000**, *33*, 791. (b) Klein, D. L.; Roth, R.; Lim, A. K. L.; Alivisatos, A. P.; McEuen, P. L. *Nature* **1997**, *389*, 699. (c) Gittins, D. I.; Bethell, D.; Schriffin, D. J.; Nichols, R. J. *Nature*, **2000**, *408*, 67. (d) Reed, M. A. *Proc. IEEE* **1999**, *87*, 652. (e) Pease, A. R.; Jeppsesn, J. O.; Stoddart, J. F.; Luo, Y. C.; Collier, C. P.; Heath, J. R. *Acc. Chem. Res.* **2001**, *34*, 433. (f) Feldheim, D. L.; Keating, C. D. *Chem. Soc. Rev.* **1998**, *27*, 1. (g) Sato, T.; Ahmed, H.; Brown, D.; Johnson, B. F. G. *J. Appl. Phys.* **1997**, 696. (h) Reed, M. A.; Zhou, C.; Muller, C. J.; Burgin, T. P.; Tour, J. M. *Science* **1997**, *278*, 252. (i) Nitzan, A. *J. Phys. Chem. A* **2001**, *105*, 2677−2670. (j) Segal, D.; Nitzan, A.; Davis, W. B.; Wasielewski, M. R. Ratner, M. A. *J. Phys. Chem. B* **2000**, *104*, 3817−3829.

(2) (a) Wuelfing, W. P.; Green, S. J.; Cliffel, D. E.; Pietron, J. J.; Murray, R. W. *J. Am. Chem. Soc.* **2000**, *122*, 11465. (b) Brust, M.; Bethall, D.; Kiely, C. J.; Schiffrin, D. J. *Langmuir* **1998**, *15*, 5425−5429.

(3) (a) Templeton, A. C.; Wuelfing, W. P.; Murray, R. W. *Acc. Chem. Res.* **2000**, *1*, 27. (b) Templeton, A. C.; Hostetler, M. J.; Warmoth, E. K.; Chen, S.; Hartshorn, C. M.; Krishnamurthy, V. M.; Forbes, M. D. E.; Murray, R. W. *J. Am. Chem. Soc.* **1998**, *120*, 4845−4849.

(4) (a) Meisel, D. In *Charging and Discharging Nanoparticles*, Proceedings of the Nineteenth DOE Solar Photochemistry Research Conference, 1995. (b) Noglik, H.; Pietro, W. J. *Chem. Mater*. **1994**, *6*, 1593−1395. (c) Cordero, S. R.; Carson, P. J.; Estabrook, R. A.; Strouse, G. F.; Buratto, S. K. *J. Phys. Chem. B* **2001**, *104*, 12137−12142. (d) Shin, M.; Wang, C.; Guyot-Sionnets, P. *J. Phys. Chem. B* **2001**, *105*, 2369−2373. (e) Wang, C.; Shim, M.; Guyot-Sionnest, P. *Science* **2001**, *291*, 2390−2392.

(5) (a) Ingram, R. S.; Hostetler, M. J.; Murray, R. W.; Schaff, T. G.; Khoury, J. T.; Whetten, R. L.; Bigioni, T. P.; Guthrie, D. K.; First, P. N. *J. Am. Chem. Soc.* **1997**, *119*, 9279. (b) Chen, S.; Murray, R. W.; Feldberg, S. W. *J. Phys. Chem. B* **1998**, *102*, 9898. (c) Hicks, J. F.; Templeton, A. C.; Chen, S.; Sheran, K. M.; Jasti, R.; Murray, R. W. *Anal. Chem*. **1999**, *71*, 3703. (d) Chen, S. W.; Murray, R. W. *J. Phys. Chem. B* **1999**, *103*, 9996.

(6) (a) Chen, S.; Ingram, R. S.; Hostetler, M. J.; Pietron, J. J.; Murray, R. W.; Schaaff, T. G.; Khoury, J. T.; Alvarez, M. M.; Whetten, R. L. *Science* **1998**, *280*, 2089. (b) Whetten, R. L.; Shafigulin, M. N.; Khoury, J. T.; Schaff, T. G.; Vezmar, I.; Alvarez, M. M.; Wilkinson, A. *Acc. Chem. Res.* **1999**, *32*, 397. (c) Schaaff, T. G.; Shafigullin, M. N.; Khoury, J. T.; Vezmar, I.; Whetten, R. L.; Cullen, W.; First, P. N.; Gutierrez-Wing, C.; Ascensio, J.; Jose-Yacaman, M. J. *J. Phys. Chem. B* **1997**, *101*, 7885−7891.

(7) (a) Zamborini, F. P.; Hicks J. F.; Murray, R. W. *J. Am. Chem. Soc.* **2000**, *122*, 4514. (b) Templeton, A. C.; Cliffel, D. E.; Murray, R. W. *J. Am Chem. Soc*. **1999**, *121*, 7081.

(8) (a) Hostetler, M. J.; Wingate, J. E.; Zhong, C.-J.; Harris, J. E.; Vachet, R. W.; Clark, M. R.; Londono, J. D.; Green, S. J.; Stokes, J. J.; Wignall, G. D.; Glish, G. L.; Porter, M. D.; Evans, N. D.; Murray, R. W. *Langmuir* **1998**, *1*, 17 (b) Chen, S. W.; Murray, R. W. *Langmuir* **1999**, *15*, 682−689.

(9) *Molecular Design of Electrode Surfaces*; Murray, R. W., Ed.; Wiley & Sons: New York, 1992.

(10) (a) Smalley, J. F.; Feldberg, S. W.; Chidsey, C. E. D.; Linford, M. R.; Newton, M. D.; Liu, Y.-P. *J. Am. Chem. Soc.* **1995**, *117*, 13141. (b) Sachs, S. B.; Dudek, S. P.; Hsung, R. P.; Sita, L. R.; Smalley, J. F.; Newton, M. D.; Feldberg, S. W.; Chidsey, C. E. D. *J. Am. Chem. Soc.* **1997**, *119*, 10563−10564. (c) Chidsey, C. E. D. *Science* **1991**, *251*, 920. (d) Creager, S.; Yu, C. J.; Bamdad, C.; O'Conner, S. O.; MacLean, T.; Lam, E.; Chong, Y.; Lou, J.; Gozin, M.; Kayyem, J. F. *J. Am. Chem. Soc*. **1999**, *121*, 1059. (e) Slowinski, K.; Fong, H. K. Y.; Majda, M. *J. Am. Chem. Soc.* **1999**, *121*, 7257−7261. (f) Holmlin, R. E.; Haag, R.; Chabinyc, M. L.; Ismagilov, R. F.; Cohen, A. E.; Terfort, A.; Rampi, M. A.; Whitesides, G. M. *J. Am. Chem. Soc.* **2001**, *123*, 5075−5085, and refs therein.

(11) Cheng, J.; Szabo, G. S.; Tossell, J. A.; Miller, C. J. *J. Am. Chem. Soc.* **1996**, *118*, 680.

(12) (a) Marcus, R. A. *Angew. Chem., Int. Ed. Engl.* **1993**, *32*, 1111. (b) Marcus, R. A., Sutin, N. *Biochim. Biophys. Acta* **1985**, *811*, 265. (c) Newton, M. D. *Chem. Rev.* **1991**, *91*, 767.

(13) (a) Hostetler, M. J.; Green, S. J.; Stoeks, J. J.; Murray, R. W. *J. Am. Chem. Soc*. **1996**, *118*, 4212−4213. (b) Green, S. J.; Stokes, J. J.; Hostetler, M. J.; Pietron, J. J.; Murray, R. W. *J. Phys. Chem. B* **1997**, *101*, 2663−2668. (c) Hostetler, M. J.; Templeton, A. C.; Murray, R. W. *Langmuir* **1999**, *15*, 3782.

(14) Brust, M.; Walker, M.; Bethell, D.; Schiffrin, D. J.; Whyman, R. *J. Chem. Soc., Chem. Commun.* **1994**, 801−802.

(15) Luedtke, W. D.; Landman, U. *J. Phys. Chem. B* **1998**, *102*, 656.

(16) Terrill, R. H.; Postlethwaite, T. A.; Chen, C.-C.; Poon, C -D.; Terzis, A.; Chen, A.; Hutchison, J. E.; Clark, M. R.; Wignall, G.; Londono, J. D.; Superfine, R.; Falvo, M.; Johnson, C. S.; Samulski, E. T.; Murray, R. W. *J. Am. Chem. Soc*. **1995**, *117*, 12537.

(17) Calculated using Hyperchem software.

(18) Pietron, J. J.; Hicks, J. F.; Murray, R. W. *J. Am. Chem. Soc*. **1999**, *121*, 5565−5570.

(19) There is a hint in Figures 3 and 6 that E_A decreases at lowered temperature; this was not pursued further in the present study.

(20) (a) Sosnoff, C. S.; Sullivan, M.; Murray, R. W. *J. Phys. Chem.* **1994**, *98*, 13643. (b) Terrill, R. H.; Hutchinson, J. E.; Murray, R. W. *J. Phys. Chem. B* **1997**, *101*, 1535.

(21) Hicks, J. F.; Zamborini, F. P.; Osisek, A. J.; Murray, R. W. *J. Am. Chem. Soc.* **2001**, *123*, 7048−7053.

(22) (a) It was also shown in ref 2a (Table 4) that so-called granular metal, or cermet, theory is not successful (predicting activation energies and producing values much larger than experiment) when it is recognized that MPC conduction is in the "low field" regime of this model, so that experimental barrier energies should be taken from a $T^{-1/2}$ and not[24b] a T^{-1} activation plot. (b) Brust, M.; Bethell, D.; Schiffrin, D. J.; Kiely, C. J. *Adv. Mater. (Weinheim, Ger)* **1995**, *7*.

(23) *CRC Handbook of Chemistry and Physics*, 72nd ed.; Lide, D. R.; Ed; CRC Press: Boca Raton, FL, 1992.

(24) Porter, M. D.; Bright, T. B.; Allara, D. L.; Chidsey, C. E. D. *J. Am. Chem. Soc.* **1987**, *109*, 3559.

(25) Hostetler, M. J.; Templeton, A. C.; Murray, R. W. *Langmuir* **1999**, *15*, 3782−2789.

(26) Modeling the shape of a Au_{309} MPC as a sphere with radius 1.1 nm shows that approximately 5 thiolate ligands would be involved with interdigitation per side or 10 ligands total. In the Au_{976} sample, approximately 10 ligands per side or 20 ligands total would be involved.